American Journal of Analytical Chemistry, **2012, 3, 512-517**
http://dx.doi.org/10.4236/ajac.2012.38068 Published Online August 2012 (http://www.SciRP.org/journal/ajac)

Synthesis and Characterization of $KFeP_2O_7$ Nanoparticles Implanted in Silica

Eduardo Ordóñez Regil[1*], Enrique Ordóñez Regil[2], Nidia García González[1,3], Samuel R. Barocio[4]

[1]Instituto Nacional de Investigaciones Nucleares, Departamento de Química, Centro Nuclear de México, Ocoyoacac, México
[2]Centro Interamericano de Recursos del Agua, Facultad de Ingenieria, UAEM, Laboratorio Estatal de Salud Pública, ISEM, Toluca, México
[3]Facultad de Química, Universidad Autónoma del Estado de México, Toluca, México
[4]Instituto Nacional de Investigaciones Nucleares, Departamento de Física, Centro Nuclear de México, Ocoyoacac, México
Email: [*]eduardo.ordonez@inin.gob.mx, samuel.barocio@inin.gob.mx, regil95@hotmail.com, nidgg@yahoo.com.mx

Received May 15, 2012; revised June 24, 2012; accepted July 2, 2012

ABSTRACT

Rivers and aquifers are increasingly affected worldwide by the action of agro-industrial pollution. Facing this challenge, nanoparticles have found a wide range of applications in the decontamination and remediation of water, given the characteristics which make them highly reactive to specific substances. One of the simplest ways of gaining access to these particles is through their synthesis over a sufficiently rigid matrix of manageable size. This report describes the synthesis and characterization of nanoparticles of iron and potassium diphosphate ($KFeP_2O_7$) synthesized on silica gel beads (SiO_2). Analysis by X-ray diffraction (XRD), scanning electron microscopy (SEM) and X-ray photoelectron spectroscopy (XPS) have been applied in order to determine the mineral phases and morphology of the synthesized compounds. Complementary tests were conducted so as to determine surface characteristics such as specific area by the BET method and point of zero charge (pH_{pzc}) by mass titration. The acid-base titration enabled to determine the adsorptive nature of nanoparticles and their response to a pH range from 1 to 12.

Keywords: $KFeP_2O_7$ Synthesis; Nanoparticles; XRD and XPS Analysis; $KFeP_2O_7$ Nanoparticles Implanted in Silica

1. Introduction

Rivers and aquifers around the world are being severely polluted by an ever expanding agro-industry. Toxic metals, in particular, represent a growing danger by accumulating in the environment and migrating to the water sources that are increasingly difficult to purify [1]. Therefore, detoxication techniques have become progressively sophisticated and more effective. The earliest studies of the reactive materials were conducted over natural minerals [2]. Later on, it was observed that the surfaces modified by chemicals enhance the extraction of pollutants in water [3]. Synthetic reactive compounds have been developed and tested in order to capture specific pollutants, as it is the case of iron derivatives like oxyhydroxides or phosphates, which have proved their efficiency in capturing cadmium or chromium in solution [4,5]. If their particle size is then reduced, the reactivity to contaminants is increased and, with it, their efficacy. Nanoparticles are used in the decontamination and remediation of water, as their characteristics make them highly reactive to specific substances. This process maximizes its effectiveness by increasing the accessibility to the surface of all the nanoparticles. In this way, the final products require a lower nanoparticle load, reducing the cost of their use [6]. However, as their management requires the use of advanced technologies due to the minute size of the particles, then the identification of an easy to apply effective technology is vital to be implemented on a large scale. One of the simplest ways of producing nanoparticles is the concomitant synthesis on a sufficiently rigid matrix, durable and of a manageable size [7]. The choice of the chemical characteristics of nanoparticles is crucial for removing a specific contaminant. For instance, metals or their salts, having intrinsic catalytic activity, are successfully used to remove specific undesirable contaminants [8-10]. Thus, iron and their salts are very effective to remove cationic species when they are in so low concentrations as to become

[*]Corresponding author.

recalcitrant with respect to usual decontamination treatments. When facing the high reactivity of the iron-potassium diphosphatethe nanoparticles, low concentrations of contaminant react with the high surface area of these particles, which turn out to be "anchored" to the surface.

2. Methodology

The substrate, composed of silica gel was reduced to an homogenous powder of 200 mesh size, which were incorporated at a 10% wt to a mixture of $NH_4H_2PO_4$ + $FeCl_3$ in a mortar, adding 10 mL of a 5M solution of KOH. This mixture was calcined in a tubular furnace at 500˚C for 2 h, with a continuous flow of water saturated air. After the completion of this operation, the material was washed with abundant distilled water until a constant pH was attained (**Figure 1**).

The dry $KFeP_2O_7/SiO_2$, which will be named hereinafter as KFP10, was subjected to physical characterization tests as follows. The mineralogical nature was identified by analyzing X-ray diffraction (XRD) patterns. The Imaging and topography of SiO_2 particles and $KFeP_2O_7$ nanoparticles were observed as electronic micrographs by means of Scanning electron microscopy (SEM) at various magnification rates. An EDS microprobe coupled to the device was used as to determine the elemental chemical composition of the samples. The presence of desired compounds was confirmed by measuring the binding energy of elements with their neighbors by means of X-ray spectroscopy (XPS) [11,12].

The specific area was measured following the N2 Brunauer-Emmett-Teller (BET) method.

In order to determine the surface characteristics the KFP10, the following techniques were applied as the suspension made of a KFP10 and $NaClO_4$ 0.5 M solution developed the solid/liquid interface. The point of zero charge (pH_{pzc}) method enabled to determine the pH at the equilibrium point of a suspension with different weight/volume ratios after a shaking period [13]. The acid-base titration revealed the behavior of the solid surface in front of a wide pH range in the solution [14].

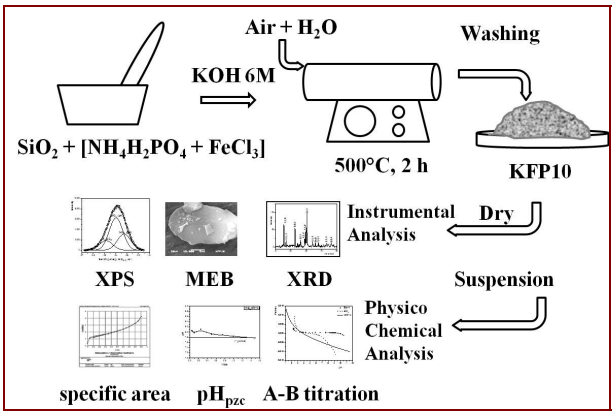

Figure 1. Experimental setup of $KFeP_2O_7/SiO_2$ synthesis.

3. Experimental

3.1. Surface Area Determination

The N2 Brunauer-Emmett-Teller (BET) method was performed on a Micromeritrics Gemini 2360 surface area analyzer. Thus, 0.5 g dry and degassed samples were analysed applying a multipoint N2 adsorption-desorption method at room temperature yielding a multipoint isotherm.

X-ray diffraction patterns were obtained by means of a diffractometer D-5000 Siemens using a copper anode (λ = 1.543 Å). The K_α radiation was selected with a diffracted beam monochromator. The XRD peaks were measured in the 2θ range of 4˚ to 70˚.

3.2. Scanning Electron Microscopy

SEM was performed on a JEOL 5900LV scanning electron microscope at 25 kV. The samples were mounted on an aluminum holder with carbon conductive tape and later covered with a gold layer, approximately 150 Å thick, using a Denton Vacuum Desk II platter. In all cases, the images were obtained using a backscattered electron detector. The elemental chemical composition of the samples was determined through Energy Dispersion Spectroscopy (EDS) on an EDAX-4 spectrometer.

3.3. X-Ray Photoelectron Spectroscopy

The spectra were collected in a K-alpha® Thermo Scientific instrument where the powdered samples were held on a copper plate at a 10^{-9} torr vacuum. Spectra were obtained using a multidetection electron analyzer and an unmonochromatized AlK_α source. The most characteristic peaks of the surveyed spectrum were recorded in narrow ranges of 30 eV binding energy.

3.4. The Following Techniques Were Applied So as to Determine the Surface Characteristics

1) The specific area was estimated following the N2 Brunauer-Emmett-Teller (BET) method on a Micromeritrics Gemini 2360 surface area analyzer. The dry and degassed samples were then analysed applying a multipoint N2 adsorption-desorption method at room temperature.

2) The point of zero charge (pH_{pzc}), was established by mass titration experiments according to the experimental procedure described by Noh and Schwartz [12]. Different amounts of KFP10 were weighed in 0.01, 0.05, 0.1, 0.2, 0.5, 1.0, 1.5 and 2 g batches which were placed in polypropylene tubes containing 10 mL of water. The resulting suspension was mixed for 24 h to allow the hydration of the solid surface before centrifugation at 3500 rpm for 15

min. The pH values of the supernatants were then measured and verified to have reached a constant value.

3) The Acid-base titration response of the surface was determined by the classical method. The titration was carried out on the aged suspension by adding incremental volumes of a base (0.1 M NaOH solution) at time intervals in accordance with the pH equilibrium. The resulting graph shows the activity of the species on the surface with the titrating acidic solution (free protons) as a function of pH.

4. Results and Discussion

Once the $KFeP_2O_7$ synthesis over SiO_2 has been conducted as described above, the resulting material was evaluated by physical and chemical analyses.

4.1. X-Ray Diffraction Analysis

Figure 2(a) shows the experimental KFP10 spectrum, where the SiO_2 gel is revealed by a wide band matching the JCPDF 01-071-0261 data card. The subjacent peaks were isolated and plotted again within the 2θ zone from 10 to 50 degrees. The peaks were in coincidence with those catalogued on the JCPDF 01-084-1798 data card. (**Figure 2(b)**).

In addition to the good matching of the spectrum, it was necessary to ensure the right interpretation of the compounds found on the silica surface. Thus, a model was developed on the basis of bibliographic data.

The structure of $KFeP_2O_7$ was represented as a three-dimensional single crystal of monoclinic symmetry of the P $2_{1/c}$ space group (**Figure 3(a)**) whose cell parameters were: a = 7.352; b = 9.987; c = 8.187 Å, β = 106.49˚, corresponding to a low temperature form. The adaptation of the diphosphate groups $[P_2O_7]$ to the octahedral $[ZrO_6]$ framework and the layered disposition of tetrahedra and octahedra lead to the formation of tunnels. The result is a cage structure where the potassium atoms within the framework can be replaced with similar atoms by means of a cationic exchange process. This design was subjected to a XRD modeling on the basis of the CaRIne v3.2 Crystallography package. The result was very close to the experimental spectrum (See **Figure 3(b)**) [15,16].

4.2. Scanning Electron Microscopy

The micrographs of KFP10 show the morphology of SiO_2 and the distribution of $KFeP_2O_7$ nanoparticles on SiO_2. The 10000× **Figure 4(a)** shows SiO_2 as a large flat surface that embeds nanoparticles. The 20000× micrograph (**Figure 4(b)**) shows a homogeneous dispersion of the small grains over the SiO_2 surface. The elemental analysis (inset) confirmed that the composition of the small grains correspond to $KFeP_2O_7$, with sizes ranging between 50 and 250 nm.

4.3. X-Ray Photoelectron Spectroscopy

The KFP10 surface was examined by an AlK_α electron beam in order to verify the $KFeP_2O_7$ presence. The acquired XPS spectra were analyzed according to the Gaussian fitting method. The general XPS analysis shows the Si/O_2 ratio matching the silica gel bulk material (**Table 1**), although with a small excess of O_2, which is attributed to the ternary compound. The $K/Fe/P_2O_7$ on the surface is mostly made of two compounds: $KFeP_2O_7$ and another one which is close to K_2SiO_6. This compound revealed the presence of an interface complex (between SiO_2 and $KFeP_2O_7$). This complex is formed by SiO_2 and reaction products of $KFeP_2O_7$, which seem to be responsible for the implantation of nanoparticles in the bulk.

The elemental interest regions confirmed the binding energies corresponding to the above mentioned compounds, yet, the Si $2p_{3/2}$ energy binding region indicates that one more interesting compound was present. The region spreading from 101 to 107 eV was deconvoluted

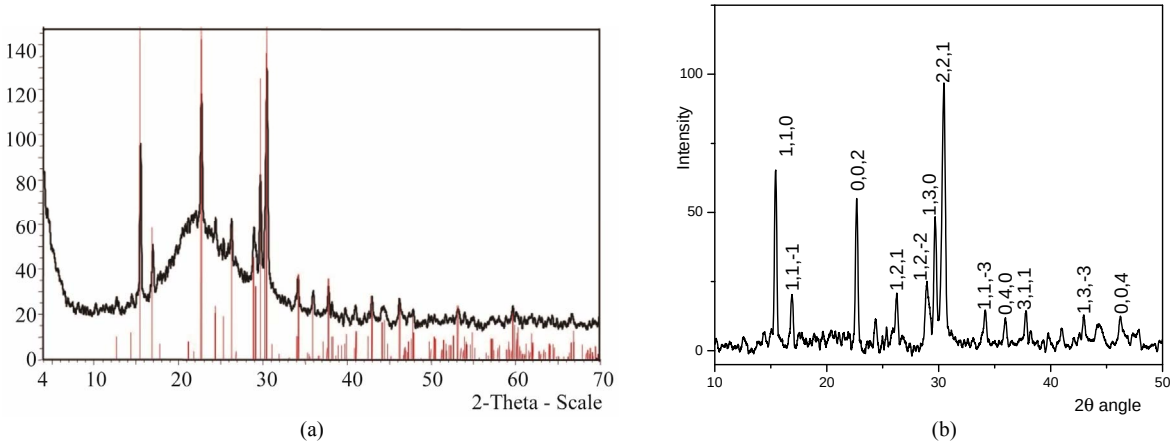

Figure 2. (a) XRD spectrum of $KFeP_2O_7/SiO_2$; (b) Detail of $KFeP_2O_7$ spectrum.

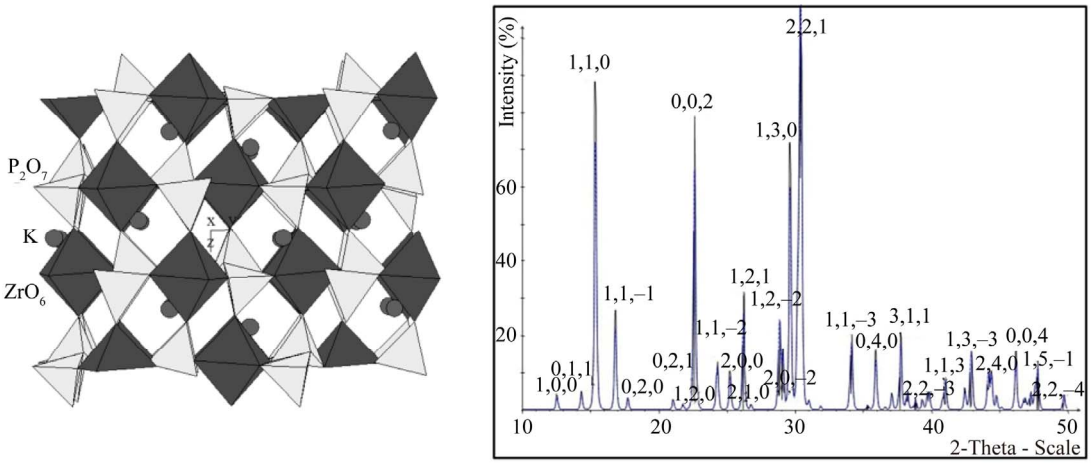

(a) (b)

Figure 3. (a) Modelled $KFeP_2O_7$ crystal; (b) Modeled XRD spectrum of $KFeP_2O_7$.

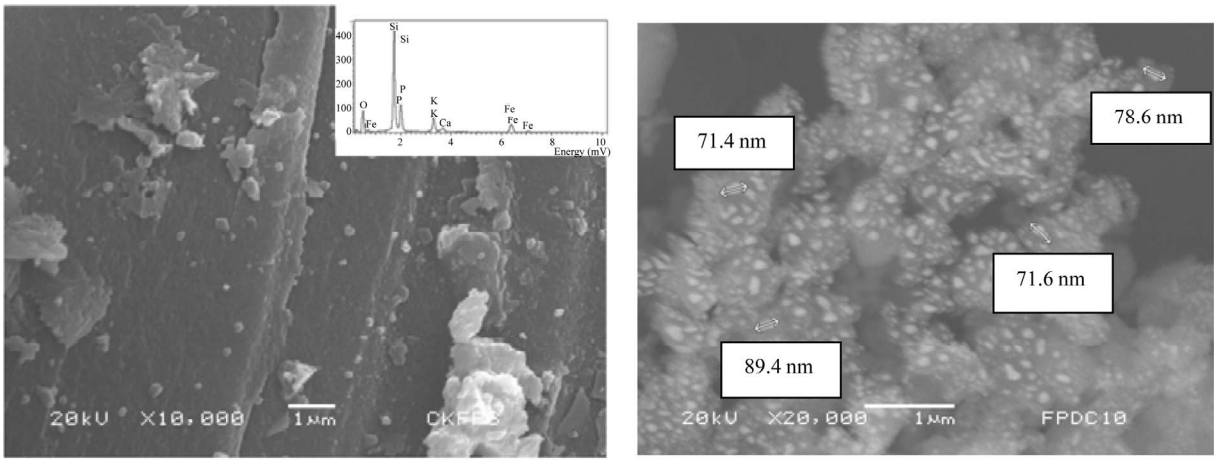

(a) (b)

Figure 4. Micrographs of SiO_2 with $KFeP_2O_7$ particles at: (a) 10000×; (b) 20000×.

Table 1. XPS survey analysis of KFP10.

Name	Peak BE	FWHM eV	Area (N)	At. %
O1s	533.12	3.17	13795.31	61.32
Si2p	104.05	2.92	6510.42	28.94
P2p	133.99	2.66	696.32	3.1
K2p	293.94	4.85	356.33	1.58
Fe2p	713.14	5.74	144.04	0.64

showing that it is composed by 3 energy peaks of 103.97, 103.26 and 104.86 eV, belonging to SiO_2 and to another compound close to K_2SiO_6. See **Figure 5**.

In all cases, it can be suggested that the particles are implanted in the bulk silicon, thus conferring on them great stability while preventing their migration to (or extraction from) the test solution, as it was proven in the contaminated water batch studies.

The results of the point of zero charge (pH_{PZC}) test for KFP10, start at pH 6. This value increases as the amount of mass grows until it reaches a plateau at pH 7.6, remaining constant, regardless the increase in mass. This asymptotic value was estimated at the equilibrium point and denotes the "the acidity of infinite mass" which is the average of the intrinsic acidity constants to each suspension.

The titration experiments performed on the silica gel and silica gel conditioned with potassium iron diphosphate nanoparticles (KFP10) enabled to determine the pH_{PZC} (**Table 2**). The decrease in SiO_2 surface area indicates that the KFP10 was implanted on its surface covering about one half of its area.

The behavior of the acid-base titration reveals that KFP10 has the property of reacting with the titrant solution (0.1 M NaOH) from its first additions, so that the dominant process is a cation reaction in which potassium is exchanged for sodium in the titrant solution. **Figure 6** exhibits the activity of the reaction equilibrium species titrated with the acid-base surface (free protons) as a

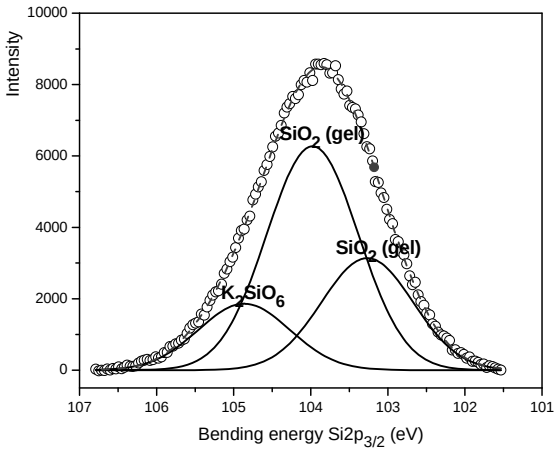

Figure 5. XPS spectra of Si $2p_{3/2}$ belonging to KFP10.

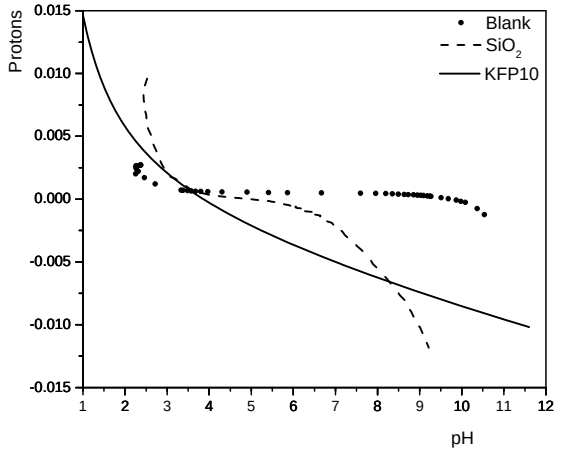

Figure 6. Acid-base titration of a blank solution, SiO_2 and KFP10, as functions of pH.

Table 2. Surface characteristics of SiO_2 and KFP10.

specific surface area SiO_2	point of zero charge SiO_2	specific surface area KFP10	point of zero charge KFP10
298 m^2/g	pH = 5.5	168 m^2/g	pH = 7.6

function of pH.

Furthermore, SEM micrographs over KFP10 samples coming from an A-B titration process have shown the same $KFeP_2O_7$ distribution as that in the dry samples. Thus, we did not detect any migration of nanoparticles into the solution, and the regeneration of this compound can be easily achieved by starting again the sorption process with an acidic treatment

5. Conclusion

A modification of the $KFeP_2O_7$ synthesis method with a view to obtaining nanoparticles over SiO_2 at low temperature has been achieved, enabling to develop particle sizes between 50 and 100 nm. Several analytical methods have shown that, although the bulk of the nanoparticles were incorporated to the $KFeP_2O_7$, another compound was produced on their interface, which acts as an implanting cement on silica grains. $KFeP_2O_7$ nanoparticles were well distributed throughout the surface of the silica, and, as the surface area is very large, it can provide a high sorption capacity for cations in solution. Furthermore, it was noticed that after the process of titration, the nanoparticles were maintained at their original place. On its part, the surface characteristics of KFP10 show a high reactivity over a wide pH range, due to the potassium cation exchange.

6. Acknowledgements

The authors are grateful to Jorge Pérez for MEB imaging and to Isidoro Martínez for XRD spectra. This study was conducted as part of the project CB 907 of ININ.

REFERENCES

[1] J. González, "Evaluation of the Impact of Climatic Change on the Economic Value of Land in Agricultural," *Journal of Agricultural Research*, Vol. 68, 2007, pp. 56-68.

[2] S. M. Robinson and J. R. Parrott Jr., "Pilot-Scale Demonstration of Process Wastewater Decontamination Using Chabazite Zeolites," Technical Report, 1989, ORNL/TM-10836.

[3] I. De la Rosa-Gómez, M. T. Olguín and D. Alcántara, "Silver-Modified Mexican Clinoptilolite-Rich Tuffs with Various Particle Sizes as Antimicrobial Agents against *Escherichia coli*," *Journal of the Mexican Chemical Society*, Vol. 54, No. 3, 2010, pp. 139-142.

[4] F. Granados-Correa, N. G. Corral-Capulin, M. T. Olguin and C. A. Acosta-Leon, "Comparison of the Cd(II) Adsoption Process between Boehmite (γ-AlOOH) and Goethite (α-FeOOH)," *Chemical Engineering Journal*, Vol. 171, No. 3, 2011, pp. 1027-1034. doi:10.1016/j.cej.2011.04.055

[5] F. Granados-Correa and J. Serrano-Gomez, "Removal of Chromium Hexavalentions from Aqueous Solution by Retention onto Iron Phosphate," *Journal of the Chilean Chemical Society*, Vol. 3, 2010, pp. 283-287.

[6] J. Kreuter, "Nanoparticles—A Historical Perspective," *International Journal of Pharmaceutics*, Vol. 331, 2007, pp. 1-10.

[7] R. Barrena, E. Casals, J. Colón, X. Font, A. Sánchez and V. Puntes, "Evaluation of the Ecotoxicity of Model Nanoparticles," *Chemosphere*, Vol. 75, No. 7, 2009, pp. 850-857. doi:10.1016/j.chemosphere.2009.01.078

[8] T. Mathialagan and T. Viraraghavan, "Adsorption of Cadmium from Aqueous Solutions by Vermiculite," *Separation Science and Technology*, Vol. 38, No. 1, 2003, pp. 57-76. doi:10.1081/SS-120016698

[9] K. Sasakia, H. Nakano, W. Wilopo, Y. Miura and T. Hirajima, "Sorption and Speciation of Arsenic by Zero-Valent Iron," *Colloids and Surfaces A*: *Physicochemical*

and Engineering Aspects, Vol. 347, No. 1-3, 2009, pp. 8-17. doi:10.1016/j.colsurfa.2008.10.033

[10] A. S. de Dios and M. E. Díaz-García, "Multifunctional Nanoparticles: Analytical Prospects," *Analytica Chimica Acta*, Vol. 666, No. 1-2, 2010, pp. 1-22. doi:10.1016/j.aca.2010.03.038

[11] B. F. Alfonso, J. A. Blanco, M. T. Fernández-Díaz, C. Trobajo , S. A. Khainakov and J. R. García, "On the Crystal Structure and Thermal Decomposition of Ammonium-Iron(III) Bis (Hydrogenphosphate)," *Dalton Transactions*, Vol. 39, No. 7, 2010, pp. 1791-1796. doi:10.1039/b912427f

[12] J.-W. Huang, P. Su, W.-W. Wu and X.-H. Wu, "Preparation and Characterization of Nanocrystalline $KFeP_2O_7$ via Solid-State Reaction at Low Heat," *Applied Chemical Industry*, Vol. 40, 2011.

[13] J. S. Noh and J. A. Schwartz, "Estimation of the Point of Zero Charge [pzc] of Simple Oxides by Mass Titration," *Journal of Colloid and Interface Science*, Vol. 130, No. 1, 1989, pp. 157-164. doi:10.1016/0021-9797(89)90086-6

[14] L. C. Bell, A. M. Posner and J. B. Quirk, "The Point of Zero Charge of Hydroxyapatite and Fluorapatite in Aqueous Solutions," *Journal of Colloid and Interface Science*, Vol. 42, No. 2, 1973, pp. 250-256. doi:10.1016/0021-9797(73)90288-9

[15] M. Gabelica-Robert, M. Goreaud, Ph. Labbe and B. Raveau, "The Pyrophosphate $NaFeP_2O_7$: A Cage Structure," *Journal of Solid State Chemistry*, Vol. 45, No. 3, 1982, pp. 389-395. doi:10.1016/0022-4596(82)90184-0

[16] D. Riou, P. Labbe and M. Goreaud, "The Diphosphate $KFeP_2O_7$: Structure and Possibilities for Insertion in the Host Framework," *Revue Chimie Minérale*, Vol. 25, No. 2, 1988, pp. 215-229.

